Electronic Supplementary Information

Binding interactions and FRET between bovine serum albumin and various phenothiazine-/anthracene-based dyes: A structure-property relationship

Shouvik Bhuin, Sayantan Halder, Subit Kumar Saha,* and Manab Chakravarty*

Department of Chemistry, Birla Institute of Technology and Sciences-Pilani, Hyderabad campuses, Hyderabad-500078, Telangana. India

Email: manab@hyderabad.bits-pilani.ac.in, sksaha@hyderabad.bits-pilani.ac.in

Table of content

General remarks

All syntheses were consummated in hot air oven-dried glassware and under inert N_2-atmoshphere. Column chromatography was accomplished using 100–200 mesh silica gel. Reactions were perfected by thin-layer chromatography on precoated silica gel 60 F254 plates (Merck & Co.) and were visualized under UV light (254 nm and 365 nm mainly). The ^1H, ^{13}C NMR spectra were recorded in $CDCl_3$ solution by using Bruker Avance DRX (400 and 100 MHz consecutively). The deuterated chloroform solvent was used, having the signals at 7.26 ppm in ^{1} H NMR and 77.16 ppm in ^{13}C- NMR as referred to TMS. Chemical shifts were reported in ppm, and multiplicities are indicated by s (singlet), d (doublet), t (triplet), m (multiplet) and dd (doublet of a doublet). ESI-LCMS was recorded in Shimadzu LCMS-2020. The HR-MS analysis was performed using a Bruker-micrOTOF-Q II. Single-crystal X-ray data were cumulated on an Enraf-Nonius MACH3 or on a Bruker AXS-SMART diffractometer using Cu Kα (λ= 0.71073 Å) radiation. A direct method was applied to solve the structures which were further refined by full-matrix least-squares method following standard procedures. [(a) Sheldrick, G. M. SADABS, Siemens Area Detector Absorption Correction; University of Gottingen, Germany, 1996. (b) Sheldrick, G. M.SHELXTL NT, Crystal Structure Analysis Package, version 5.10; Bruker AXS, Analytical X-ray System: Madison, WI, 1999.]. Absorption corrections were undergone using SADABS program, where applicable. Prevalently all the non-hydrogen atoms were refined anisotropically. Moreover, hydrogen atoms were fixed by geometry or located by a difference Fourier map and refined isotropically. All the bonds, bond angles or other distances and dihedral angles are determined using mercury 3.3 software.

Synthesis of 2-((10-pentyl-10H-phenothiazin-3-yl)methylene)malononitrile (C5-PTZCN)

C5-PTZA (100 mg, .34 mmol, 1 equiv.) and malononitrile (118 mg, 1.78 mmol, 5.24 equivalents) were dissolved into 10 ml Ethanolic water (6:1) medium under N_2 flow and were continued on reflux at 90^0C with continuous stirring up to 45 minutes under this inert condition. The reaction was surveiled by checking TLC by eluting it into 10% Ethyl acetate-Hexane medium. A red fluorescent spot was observed at R_f = 0.43 on full consumption of starting material aldehyde. Next, the reaction was quenched with brine water and worked up with ethyl acetate (15 mL × 2). The organic layer was allowed to be dried over anhydrous sodium sulphate and later, it was concentrated. The resulting red fluorescent molecule was separated by carrying

out a 120 mesh silica gel column chromatography with 8% Ethyl acetate-Hexane solvent mixture. Thus the separated compound was obtained as blackish red solid, mp: decomp (85-87 ^{0}C); yield 95%. IR (ν cm^{-1}, with KBr): 2361, 2340, 1798, 735, 1652, 1556, 1508, 1412, 802. ^{1}H NMR (400 MHz, $CDCl_3$): δ 7.76-7.71 (1H, m), 7.54-7.52 (1H, m), 7.48 (1H, S), 7.17 (1H, t, *J*=17.2 Hz), 7.09 (1H, dd, *J*=9.2 Hz), 7.01 (1H, t, *J*=16 Hz), 6.89 (1H, d, *J*=9.2 Hz), 6.85 (1H, d, *J*= 8.8 Hz), 3.90 (2H, t, *J*=14.8 Hz), 1.81 (2H, q), 1.45-1.39 (4H, m), .93 (t, 3H, *J*=14.4 Hz). ^{13}C NMR (100 MHz, $CDCl_3$): δ 157.3, 150.8, 142.5, 132.3, 131.4, 130.9, 129.5, 128.9, 127.8, 127.6, 125.2, 124.2, 122.2, 116.1, 114.9, 113.6, 48.2, 29.7, 28.9, 26.4, 22.7. LC-MS (ESI): m/z: [M + H]$^+$ calcd for $C_{21}H_{19}N_3S$ 346.1333, found 346.2500.

Synthesis of 2-amino-4-methyl-6-(10-pentyl-10H-phenothiazin-3-yl) isophthalonitrile (C5-PTZDCA)

Aldehyde (100mg, .34 mmol, 1 equiv.) and malononitrile (118 mg, 1.78 mmol, 5.24 equivalents) were dissolved into 10 ml of Ethanol: Water (6:1) medium under N_2 flow and were allowed to stir for 10 minutes. Later the reaction went on reflux at 90^{0}C with continuous stirring upto 45 minutes under this inert condition. The due course of the reaction was monitored by checking TLC by eluting it into 10% Ethyl acetate-Hexane medium. Once the aldehyde was consumed fully to form an intermediate 2-((10-pentyl-10H-phenothiazin-3-yl) methylene) malononitrile compound (I), the reaction was permitted to come down to room temperature. After that triethylamine (TEA, 0.24 ml, 1.7 mmol, 5 equivalent) and malononitrile (118 mg, 1.78 mmol, 5.24 equivalents) were added again to the same reaction mixture without changing the pot under inert environment and the reaction was let to proceed on refux (90^{0}C) once again for another 15 minutes. Next on TLC checking with 10% the formation of a new yellow fluorescent spot was confirmed at R_f = 0.3. The resulting reaction mixture was quenched with water, extracted with ethyl acetate (15 mL × 2), and washed with brine. The organic layer was dried over anhydrous sodium sulphate and was concentrated. The resulting highly fluorescent molecule was separated by performing a 120 mesh silica gel column chromatography with 8% Ethyl acetate-Hexane solvent mixture. Next the separated compound was dried under high vacuum and put to grow crystal using 30% Ethyl acetate-Hexane solvent medium. After completion of crystallization the solution was decanted and the compound was received as orange yellow crystal, mp (140-142 ^{0}C); yield 63%. IR (ν cm^{-1}, with KBr): 3237, 2212, 1733,

1634, 1582, 1464, 1364, 1014, 749. ^{1}H NMR (400 MHz, $CDCl_3$): δ 7.37 (1H, dd, *J*=10.8 Hz), 7.24 (1H, d, *J*=2 Hz), 7.18-7.10 (2H, m), 6.95-6.06 (3H, m), 6.64 (1H, s), 5.24 (2H, s), 3.86 (2H, t, *J*=14.4 Hz), 2.49 (3H, s), 1.82 (2H, q), 1.46-1.34 (4H, m), .90 (3H, t, *J*=14 Hz). ^{13}C NMR (100 MHz, $CDCl_3$): δ 152.7, 148.7, 147.6, 146.6, 144.4, 131.3, 127.6, 127.5, 127.4, 127.0, 125.3, 123.9, 122.9, 119.9, 116.2, 115.6, 115.5, 115.0, 96.0, 93.2, 47.6, 29.3, 29.2, 26.5, 24.5, 22.4. HRMS (ESI): m/z: $[M]^+$ calcd for $C_{26}H_{24}N_4S$ 424.1722, found 424.1714. The X-ray structure is determined for this compound. CCDC Number: 2041739.

Synthesis of 2-amino-4-(anthracen-9-yl)-6-methylisophthalonitrile (ANTDCA)

This compound was synthesised in the same way which were followed for C5-PTZDCA. Aldehyde (100mg, .48 mmol, 1 equiv.) and malononitrile (167 mg, 2.54 mmol, 5.24 equivalents) were taken to dissolve into 10 ml of Ethanol: Water (6:1) medium under N_2 flow and were stirred for 10 minutes. Next the reaction was permitted to undergo on reflux at 90^0C with continuous stirring upto 45 minutes under this inert condition. The progression of the reaction was observed by checking TLC by eluting it into 10% Ethyl acetate-Hexane medium. Having the aldehyde ingested fully to form an intermediate 2-((10-pentyl-10H-phenothiazin-3-yl) methylene) malononitrile compound (I), the reaction was allowed to return back to room temperature. Then again triethylamine (TEA, 0.34 ml, 2.42 mmol, 5 equivalent) and malononitrile (167 mg, 2.54 mmol, 5.24 equivalents) were added to this reaction mixture without changing the pot under inert condition and the reaction was let to run on refux (90^0C) for 45 minutes once more. A new sky-blue coloured spot was confirmed at R_f = 0.28 by dipping TLC into 10% Ethyl Acetate-Hexane medium. The ensued reaction mixture was quenched with water, extracted with ethyl acetate (15 mL × 2), and washed with brine. The organic layer was concentrated after drying over anhydrous sodium sulphate. A column chromatography was performed by using a 120 mesh silica gel with 8% Ethyl acetate-Hexane solvent mixture to separate the sky-blue fluorescent spot. Next the isolated compound was dried under high vacuum and put to grow crystal using 10% Ethyl acetate-Hexane solvent medium. After crystallization the solution was decanted and the compound was received as yellow crystal, decomp. (210-213 ^{0}C); yield 25%. IR (ν cm^{-1}, with KBr): 3242, 2215, 1650, 1620, 1578, 1513, 1465, 1442, 1376, 1287, 1155, 824. ^{1}H NMR (400 MHz, $CDCl_3$): δ 8.57 (1H, s), 8.08 (2H, d, *J*= 9.2 Hz), 7.51-7.47 (4H, m), 7.45 (1H, d, J=1.2 Hz), 7.43-7.41 (1H, m), 6.76 (1H, s), 5.28 (2H, s), 2.6 (3H, s). ^{13}C

NMR (100 MHz, $CDCl_3$): δ 152.1, 148.3, 147.9, 131.2, 131.0, 129.4, 128.8, 128.7, 126.7, 125.4, 125.1, 122.8, 115.3, 114.9, 97.8, 97.3, 21.5. HRMS (ESI): m/z: $[M + H]^+$ calcd for $C_{23}H_{15}N_3$ 334.1300, found 334.1335. The X-ray structure is determined for this compound. CCDC Number: 2041742.

Note S1: Fractional accessibility of a quencher

The modified Stern-Volmer equation (Equation S1) is

$$\frac{F_o}{(F_o - F)} = \frac{1}{f_a K_a [DMASBT]} + \frac{1}{f_a}$$

(S1)

where F_o and F are the total fluorescence intensities of Trp residues of BSA in the absence and presence of the dye, respectively. K_a is the S-V quenching constant for the quenching of accessible fraction f_a can be written as (Equation S2):

$$f_a = \frac{F_{0a}}{F_{0b} + F_{0a}}$$

(S2)

where the subscript 0 refers to the fluorescence intensity in the absence of quencher. Thus, F_{0a} denotes the fluorescence intensity from the accessible fraction, while F_{0b} refers to the fluorescence intensity from the buried fraction in BSA both in the absence of a quencher.

Note S2: Calculation of number of binding sites (*n*) and binding constant (*K′*)

By assuming the static quenching and independent binding sites for BSA in case of a static quenching, there are three different methods (Method 1, Method 2, and Method 3) to estimate the binding constant K' and the number of binding sites (n).[1] However, in Method 1, the free concentration of quencher has been replaced by the total concentration of quencher, and in Method 2, all concentrations are replaced by the equivalent concentrations. On the other hand, in Method 3, no assumed conditions about concentration are desired. Thus, Method 3 has been followed in this study, and the equation used in this method for the estimation of K' and n is given below (Equation S3):

$$\log[(F_o - F)/F] = n\log K' - n\log(1/([Q] - (F_o - F)[P]/F_o)) \quad \text{(S3)}$$

where F_o and F fluorescence intensities in the absence and presence of quencher, respectively, [Q] and [P] are total concentrations of quencher and protein, respectively.

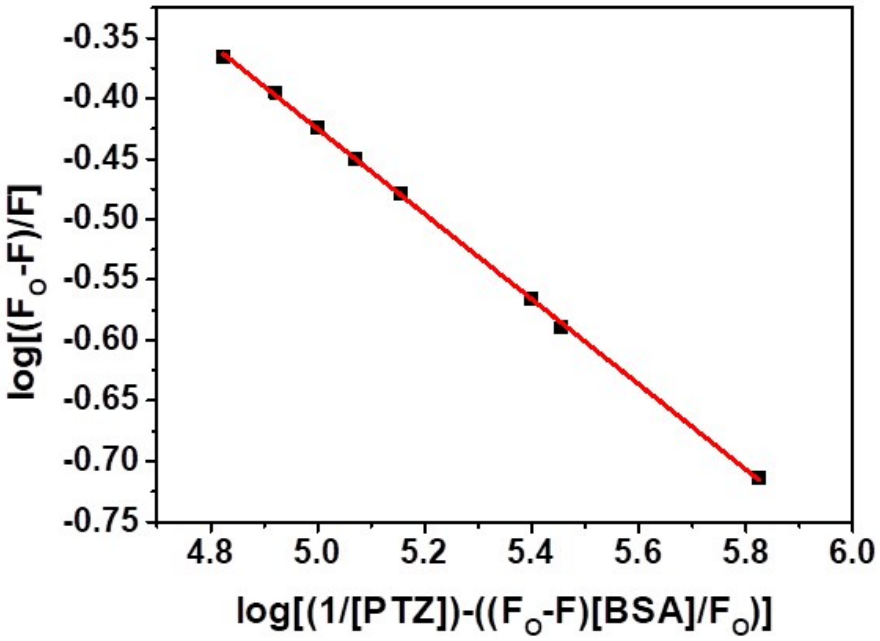

Fig. S1 log[($F_o - F$)/F] versus log(1/([**PTZ**] – ($F_o - F$)[BSA]/F_o))

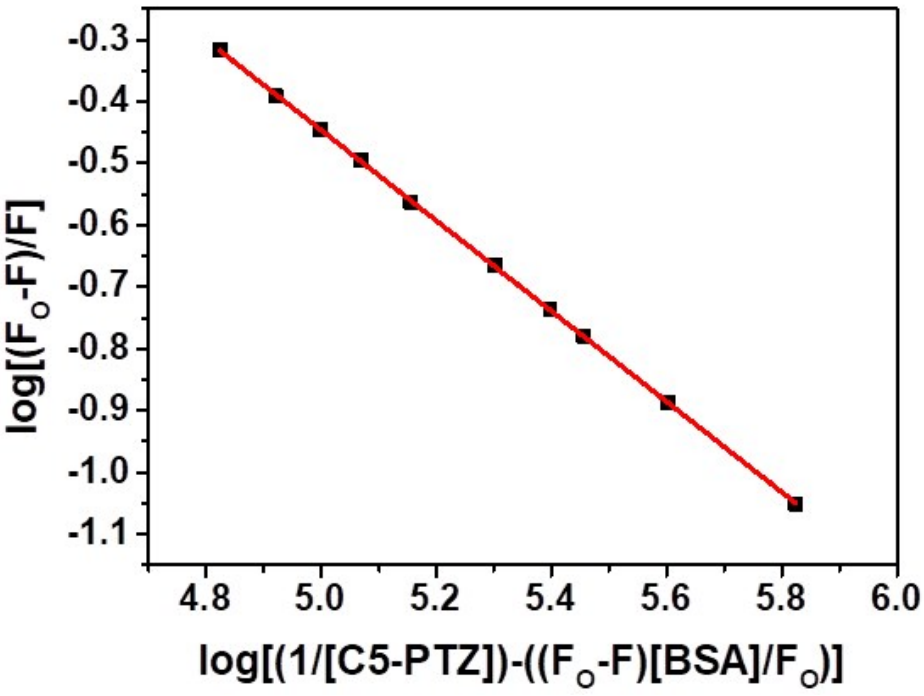

Fig. S2 log[(F_o – F)/F] versus log(1/([**C5-PTZ**] – (F_o – F)[BSA]/F_o))

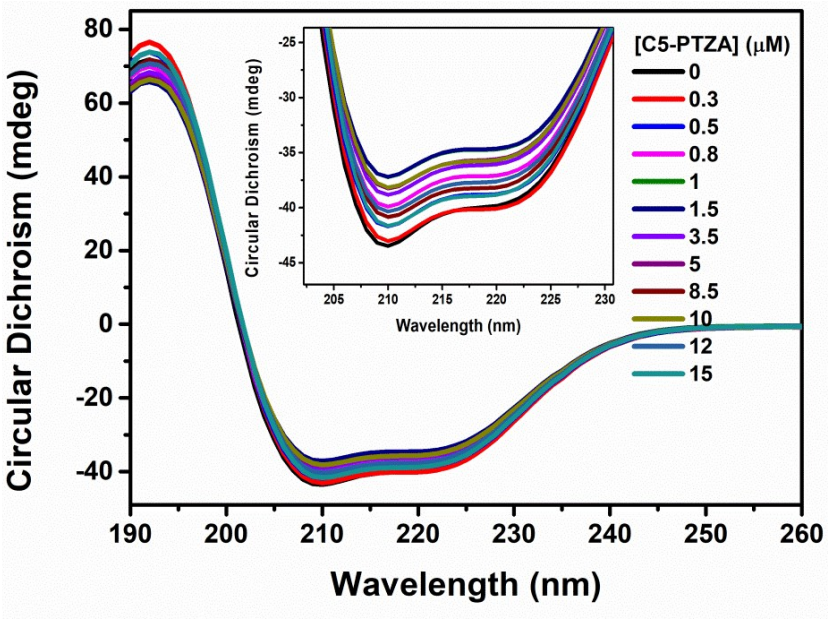

Fig. S3 Circular dichroism spectra of BSA in presence of different concentrations of C5-PTZA. Inset is for better views for changes. [BSA] = 5 μM.

Note S3: Modified Stern-Volmer equations for combined static and dynamic quenching mechanism

The modified S-V equation for a quenching process through both static and dynamic quenching can be written as Equation S4.

$$\frac{F_0}{F} = (1 + K_D[Q])(1 + K_S[Q]) \tag{S4}$$

where K_D and K_S are S-V dynamic and static quenching constants, respectively, other terms have the usual meaning. This equation can be further modified as Equation S5. This altered form of the S-V equation is second order in [Q], which accounts for the upward curvature.

$$\frac{F_0}{F} = 1 + (K_D + K_S)[Q] + K_D K_S[Q]^2 = 1 + K_{app}[Q] \tag{S5}$$

where,

$$K_{app} = \left(\frac{F_0}{F} - 1\right)\frac{1}{[Q]} = (K_D + K_S) + K_D K_S[Q] \quad \text{(S6)}$$

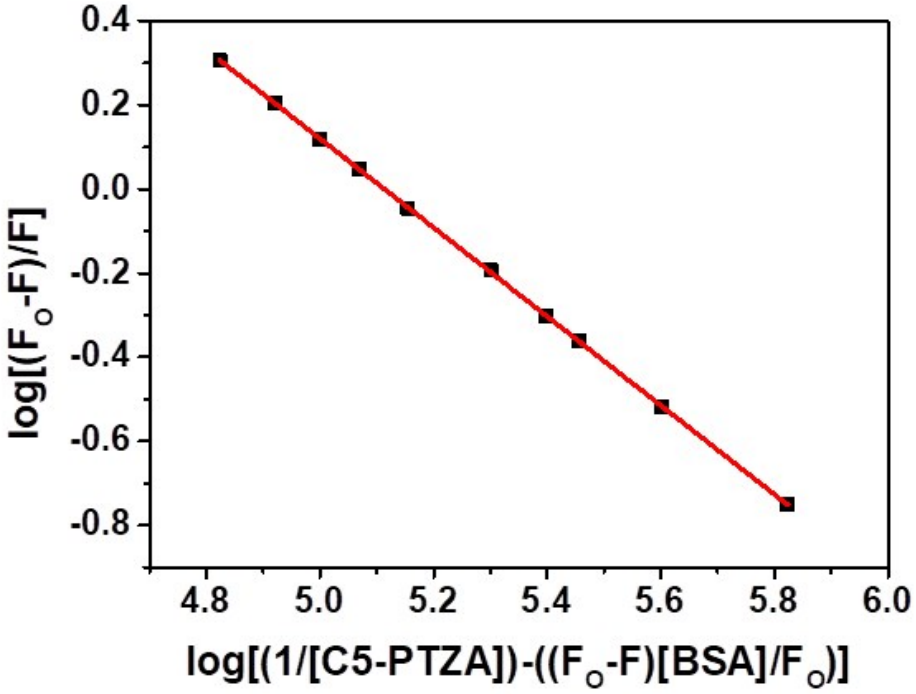

Fig. S4 log[(F_o – F)/F] versus log(1/([**C5-PTZA**] – (F_o – F)[BSA]/F_o))

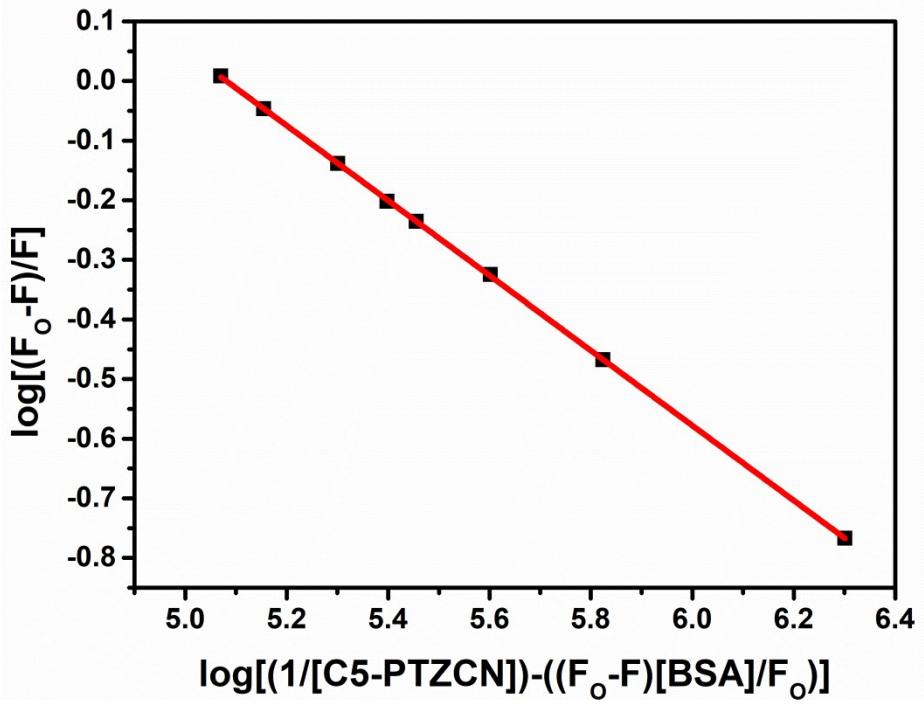

Fig. S5 log[(F_o – F)/F] versus log(1/([**C5-PTZCN**] – (F_o – F)[BSA]/F_o))

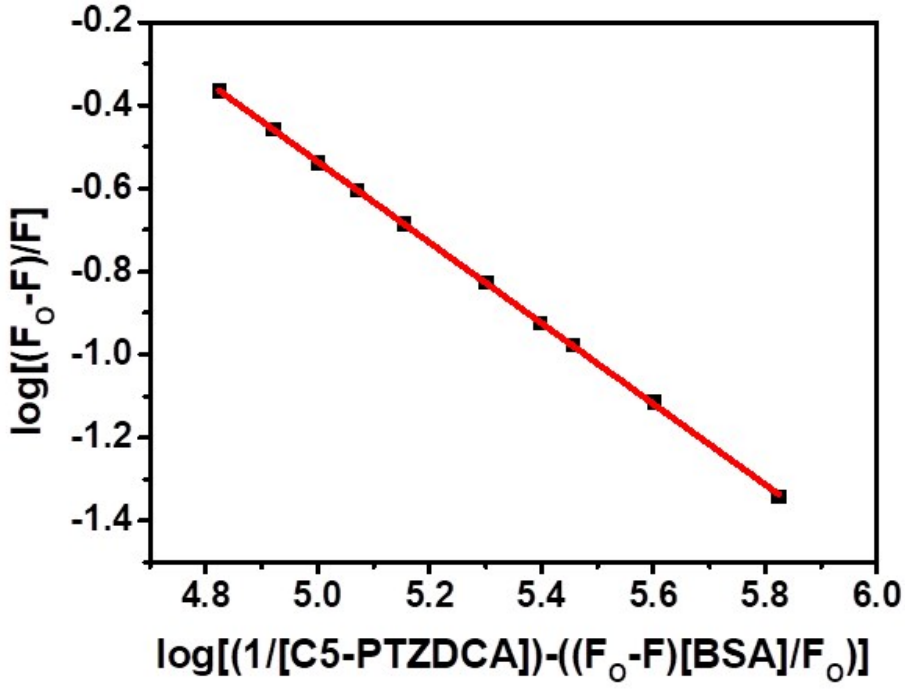

Fig. S6 log[(F_o – F)/F] versus log(1/([**C5-PTZDCA**] – (F_o – F)[BSA]/F_o))

Note S4: Sphere-of-action model – Modified Stern Volmer equation

The modified S-V equation for the sphere-of-action model is written as Equation S7.[40]

$$\frac{F_O}{F} = \left(1 + K_D[Q]\right)\left(e^{VN_{AV}[Q]/1000}\right)$$

(S7)

where V is the volume of a sphere of action = $\frac{4}{3}\pi r^3$, N_{AV} is Avogadro's number, $[Q]$ is the concentration of quencher, and K_D is S-V dynamic quenching constant. The modified form of Equation S7 is as given below (Equation S8):

$$\frac{F}{F_O} = [1/(1 + K_D[Q])]\left(e^{-VN_{AV}[Q]/1000}\right)$$

(S8)

With a target to calculate the value of V, Janosi *et al.*[2]assumed that the exponential term, $e^{-VN_{AV}[Q]/1000} \approx 1 - (VN_{AV}[Q]/1000)$ as the quantity, $VN_{AV}[Q]/1000$ is minimal because V and $[Q]$ are small, thus Equation S8 can be written as

$$\frac{F}{F_O} = \left(1 - \left(\frac{VN_{AV}[Q]}{1000}\right)\right)/(1 + K_D[Q])$$

(S9)

The simpler form of Equation S9 is as given as Equation S10 :[3,4]

$$(1 - \frac{F}{F_O})/[Q] = (F/F_O)K_D + VN_{AV}/1000$$

(S10)

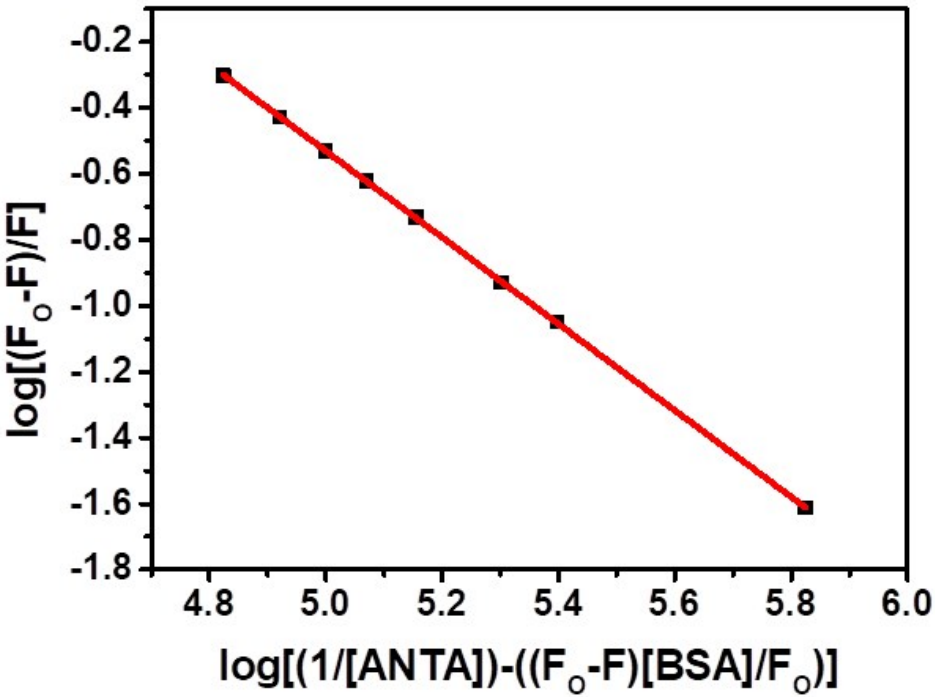

Fig. S7 $\log[(F_o - F)/F]$ versus $\log(1/([\mathbf{ANTA}] - (F_o - F)[\mathrm{BSA}]/F_o))$

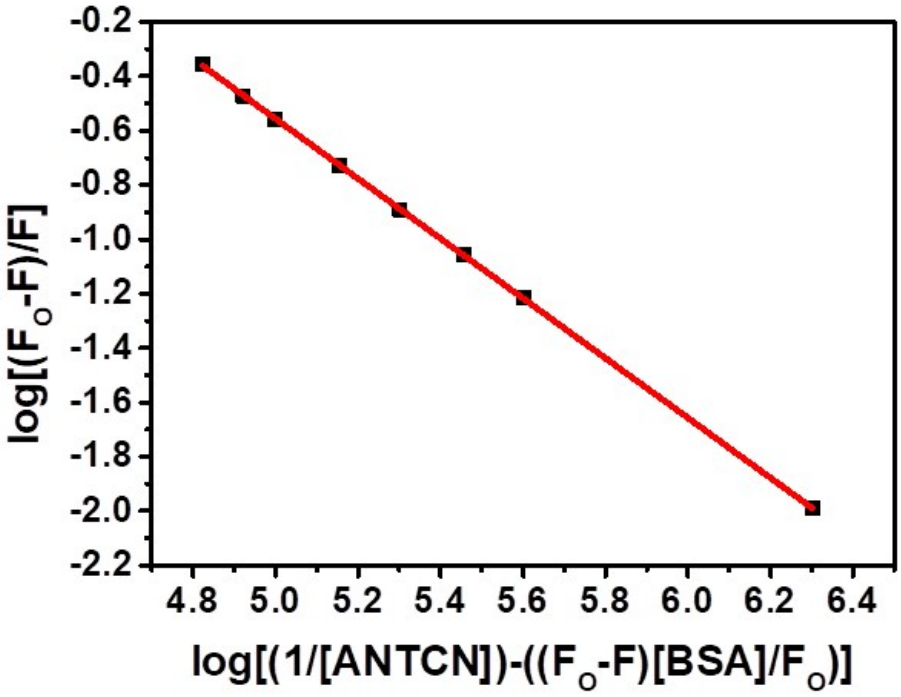

Fig. S8 $\log[(F_o - F)/F]$ versus $\log(1/([\mathbf{ANTCN}] - (F_o - F)[\mathrm{BSA}]/F_o))$

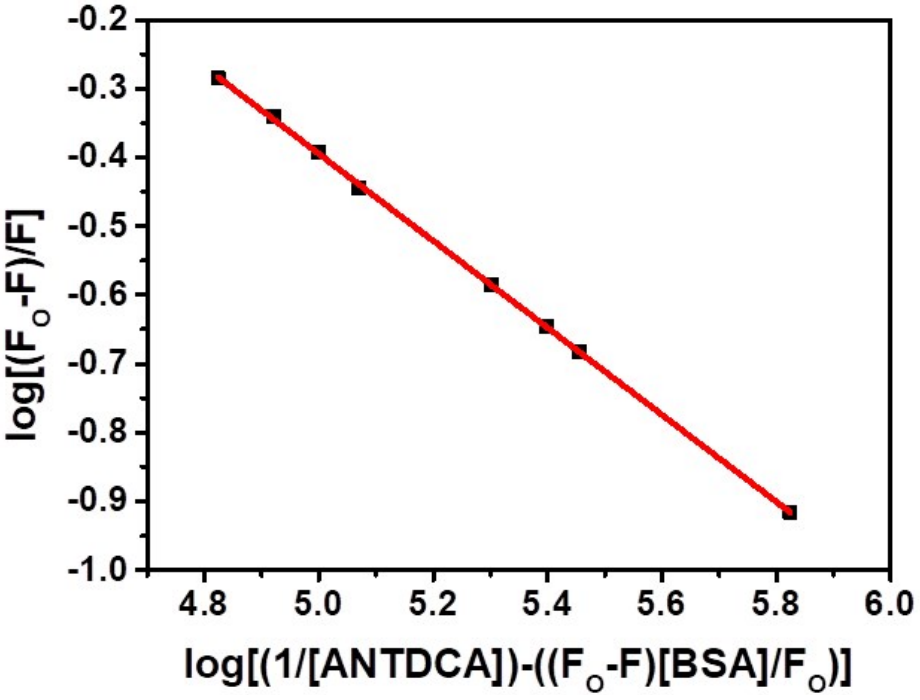

Fig. S9 $\log[(F_o - F)/F]$ versus $\log(1/([\textbf{ANTDCA}] - (F_o - F)[\text{BSA}]/F_o))$

Note S5: Details of calculation of FRET parameters and overlap integral

The FRET is a radiationless energy transfer phenomenon occurring between donor and acceptor. It finds its application in different innovative fields of research.[5–7] In the RET process, energy gets transferred from a donor to an acceptor moiety through dipole-dipole interactions without any emission and reabsorption of photons. Upon excitation of the donor, fluorescence occurs from both the donor and acceptors. With increasing concentration of acceptor, the fluorescence from the donor gets quenched.[8] According to Förster's theory, the control of the FRET efficiency depends on the following factors: (i) the extent of overlap between the donor's fluorescence and the acceptor's absorbance, (ii) the distance between the donor and the acceptor (acceptable range is ~2–9 nm),[9] and (iii) the proper orientation between the donor's and the acceptor's transition dipoles.[10] BSA possesses two Trp residues, Trp-134 and Trp-213, which act as donors in energy transfer to the other acceptor molecules.

The distance corresponding to 50% energy transfer from the donor to the acceptor takes place is called Förster's distance (R_o), which has been calculated using Equation S11 given below:

$$R_O = 0.211 \times \left[\kappa^2 \eta^{-4} Q_D J(\lambda)\right]^{1/6} \quad \text{(S11)}$$

where $J(\lambda)$ is the overlap integral and calculated following Equation S12 which measures

$$J(\lambda) = \frac{\int_0^\infty F_D(\lambda)\varepsilon_A(\lambda)\lambda^4 d\lambda}{\int_0^\infty F_D(\lambda)d\lambda} \quad \text{(S12)}$$

the magnitude of overlap, in units of $M^{-1}cm^{-1}(nm)^4$, between the emission spectrum and the absorption spectrum of donor and acceptor, respectively. The corrected fluorescence intensity of the donor and the extinction coefficient of the acceptor at a λ are represented by $F_D(\lambda)$ and $\varepsilon_A(\lambda)$, respectively.

κ^2 represents the relative orientations of the transition dipoles of the donor and acceptor in space. Its value is taken to be 2/3 by taking the average of the dynamic motions of donor and acceptor moieties. The refractive index of the medium (HEPES buffer) is represented by η with a value of 1.4, and Q_D is the quantum yield (0.042) of the donor in the absence of acceptor. The value of R_o has been determined by developing a suitable Matlab program. The efficiency of energy transfer (E_T) has been calculated using the following Equation S13.

$$E_T = 1 - \frac{F_{DA}}{F_D} \quad \text{(S13)}$$

where F_D and F_{DA} are the fluorescence intensities of Trp residues of BSA in the absence and presence of the acceptor, respectively. The average distance (r) between the dye and Trp residues of BSA has been calculated using the value of R_o and E_T following the relation (Equation S14):

$$E_T = \frac{{R_0}^6}{{R_0}^6 + r^6}$$

(S14)

Cyclic-Voltammetry (CV) plots

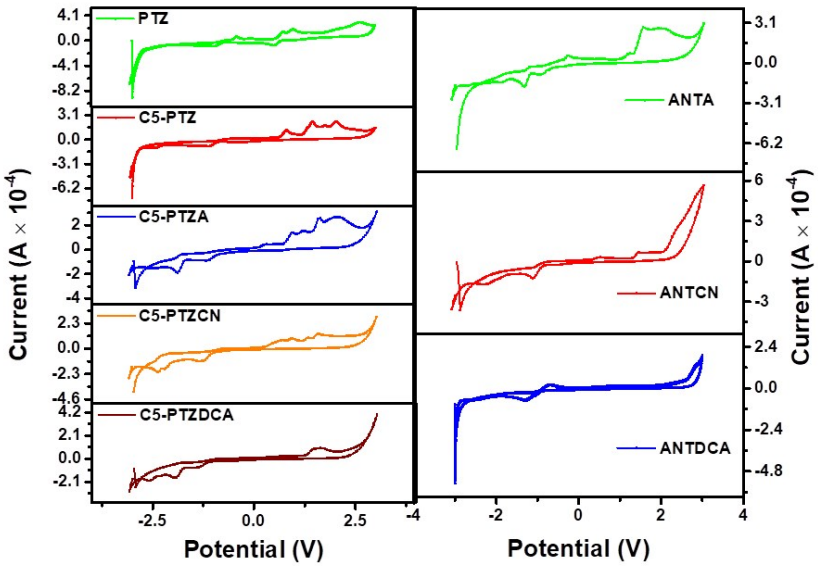

Fig. S10 CV diagrams for all dyes

The HOMO/LUMO energy levels were calculated from the onset oxidation/reduction potentials in due course of positive/negative scans. An example of this, for C5-PTZDCA as glassy carbon (GC) electrode was used as working electrode (WE) along with the Pt-wire and Ag/AgCl were used as counter electrode (CE) and reference electrode (RE) respectively with a 0.1 M tetrabutylammonium perchlorate (TBAP) in acetonitrile as electrolyte in a typical three-electrode system at normal atm,

E_{HOMO} = - (E^{onset}_{ox} - 0.49 + 4.8) eV = - (2.09 - 0.49 + 4.8) eV = 6.4 eV

E_{LUMO} = - (E^{onset}_{red} - 0.49 + 4.8) eV = - (-2.86 - 0.49 + 4.8) eV = -1.45 eV

Band Gap = E_{LUMO} - E_{HOMO} = (-1.45 + 6.4) eV = 4.95 eV

Thus the band-gaps of other dyes were determined.

NMR Spectra

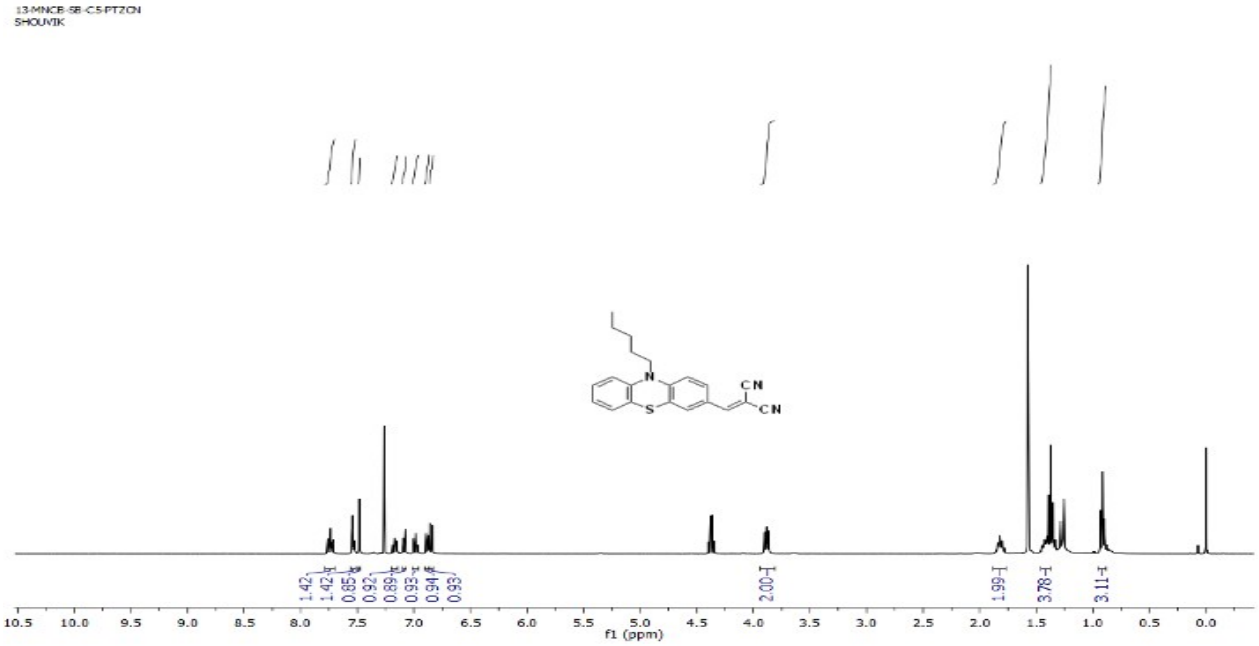

Fig. S11 ^{1}H NMR spectra of C5-PTZCN

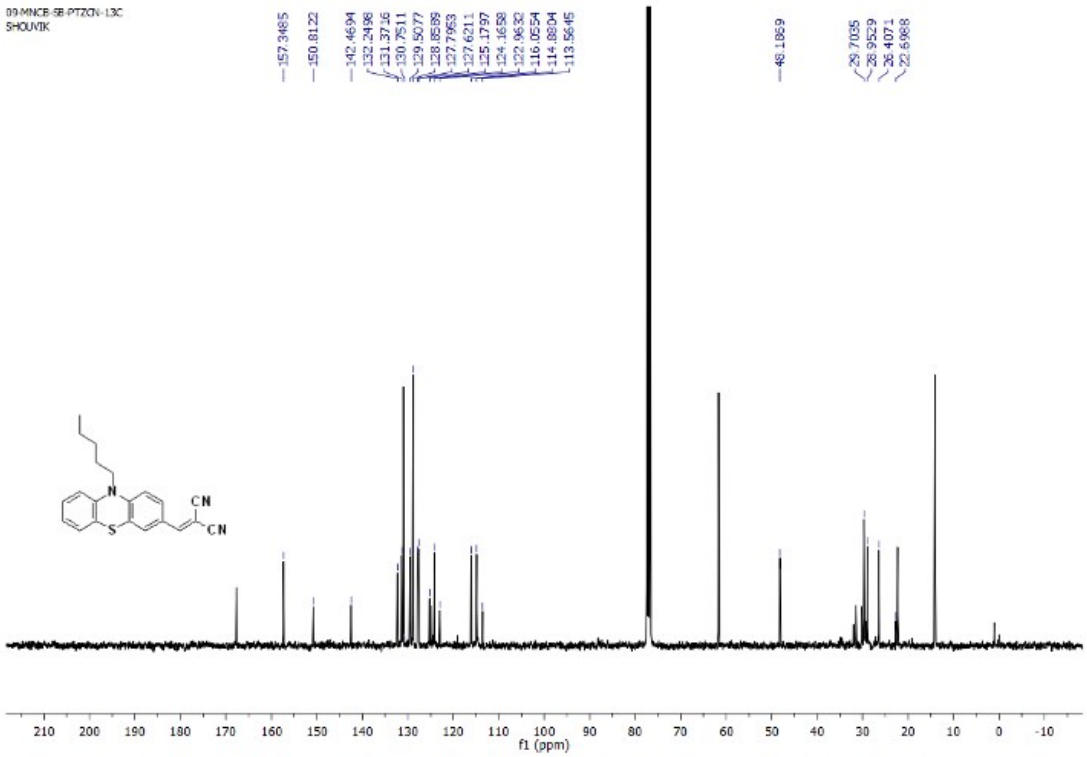

Fig. S12 ^{13}C NMR spectra of C5-PTZCN

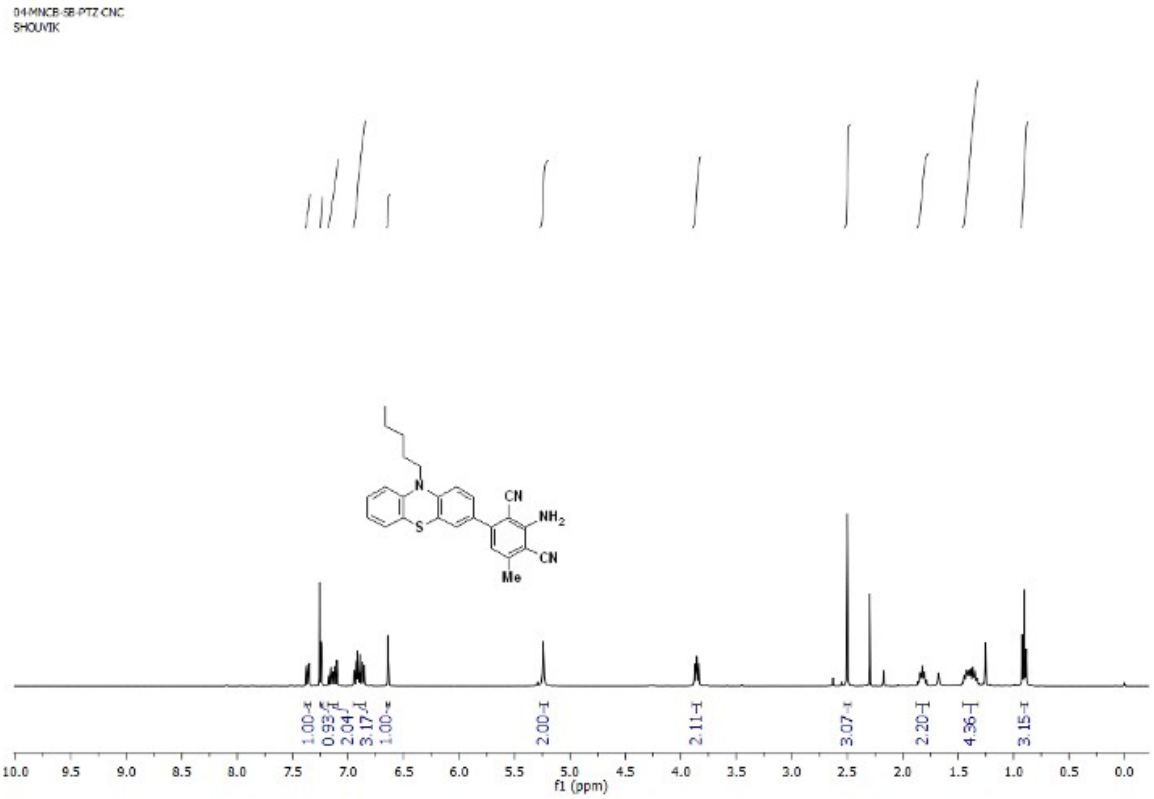

Fig. S13 ^{1}H NMR spectra of C5-PTZDCA

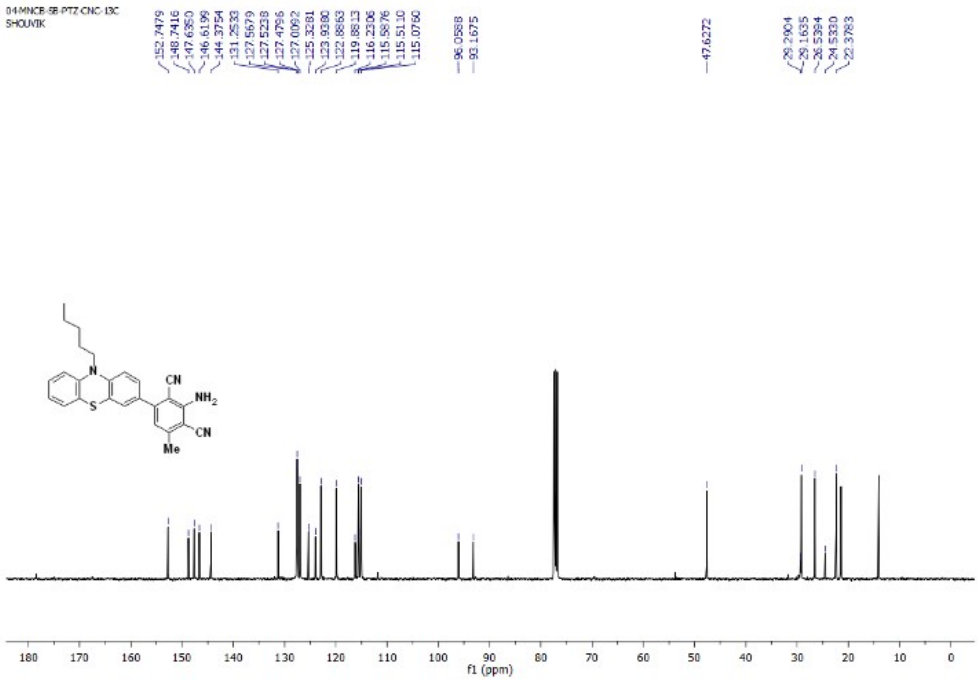

Fig. S14 ^{13}C NMR spectra of C5-PTZDCA

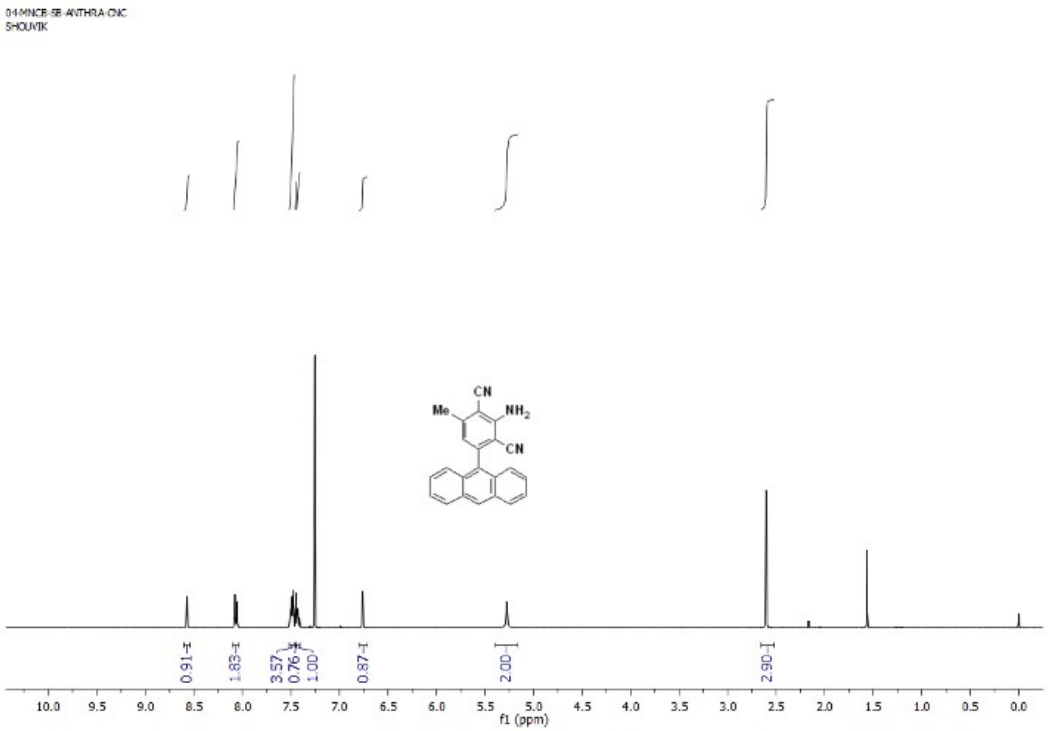

Fig. S15 ^{1}H NMR spectra of ANTDCA

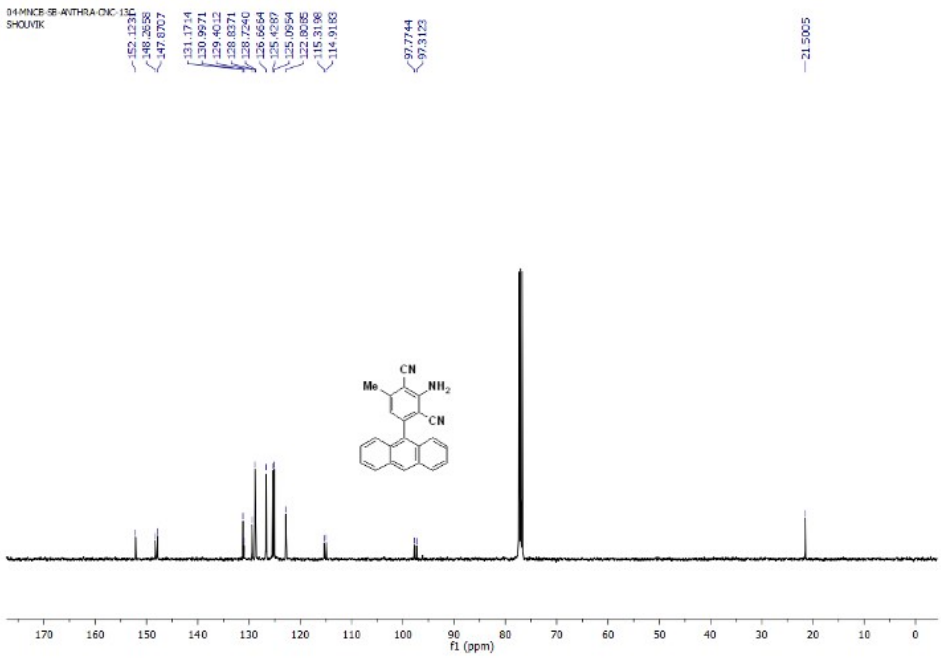

Fig. S16 ^{13}C NMR spectra of ANTDCA

References

1 S. Bi, L. Ding, Y. Tian, D. Song, X. Zhou, X. Liu and H. Zhang, Investigation of the interaction between flavonoids and human serum albumin, *J. Mol. Struct.*, 2004, **703**, 37–45.

2 T. Z. Janosi, J. Korppi-Tommola, Z. Csok, L. Kollar, P. Myllyperkio and J. Erostyak, Anthracene Fluorescence Quenching by a Tetrakis (Ketocarboxamide) Cavitand, *J. Spectrosc.*, , DOI:10.1155/2014/708739.

3 R. Giri, Fluorescence quenching of coumarins by halide ions, *Spectrochim. Acta - Part A Mol. Biomol. Spectrosc.*, 2004, **60**, 757–763.

4 J. Thipperudrappa, D. S. Biradar, M. T. Lagare, S. M. Hanagodimath, S. R. Inamdar and J. S. Kadadevaramath, Fluorescence quenching of BPBD by aniline in benzene-acetonitrile mixtures, *J. Photochem. Photobiol. A Chem.*, 2006, **177**, 89–93.

5 A. Dietrich, V. Buschmann, C. Müller and M. Sauer, Fluorescence resonance energy transfer (FRET) and competing processes in donor-acceptor substituted DNA strands: A comparative study of ensemble and single-molecule data, *Rev. Mol. Biotechnol.*, 2002, **82**, 211–231.

6 A. Ben Othman, W. L. Jeong, J. S. Wu, S. K. Jong, R. Abidi, P. Thuéry, J. M. Strub, A. Van Dorsselaer and J. Vicens, Calix[4]arene-based, Hg2+-induced intramolecular fluorescence resonance energy transfer chemosensor, *J. Org. Chem.*, 2007, **72**, 7634–7640.

7 S. Zadran, S. Standley, K. Wong, E. Otiniano, A. Amighi and M. Baudry, Fluorescence resonance energy transfer (FRET)-based biosensors: Visualizing cellular dynamics and bioenergetics, *Appl. Microbiol. Biotechnol.*, 2012, **96**, 895–902.

8 D. W. Piston and G. J. Kremers, Fluorescent protein FRET: the good, the bad and the ugly, *Trends Biochem. Sci.*, 2007, **32**, 407–414.

9 A. Chakraborty, S. Ghosh, S. Kar, D. N. Nath and N. Guchhait, Dual emission from (E)-3-(4-methylamino-phenyl)-acrylic acid ethyl ester (MAPAEE) and its application as fluorescence probe for studying micellar and protein microenvironment, *J. Mol. Struct.*, 2009, **917**, 148–157.

10 J. R. Lakowicz, Chapter 13 - Energy Transfer, *Princ. Fluoresc. Spectrosc.*, 2006, 443–475.

----------End----------